Control Engineering Practice 42 (2015) 50–59

Contents lists available at ScienceDirect

Control Engineering Practice

journal homepage: www.elsevier.com/locate/conengprac

Discrete robust switched H_∞ tracking state feedback controllers for lateral vehicle control

Menhour Lghani [a,*], Koenig Damien [b], d'Andréa-Novel Brigitte [c]

[a] Reims University, 10000 Troyes, France
[b] Laboratoire de Grenoble Images Parole Signal et Automatique, UMR CNRS-INPG-UJF, 38402 Saint Martin d'Hères, France
[c] Centre de Robotique, Mines ParisTech, PSL Research University, 60 boulevard Saint-Michel, 75272 Paris cedex 06, France

ARTICLE INFO

Article history:
Received 23 January 2014
Accepted 6 May 2015

Keywords:
Switched and uncertain linear systems
Tracking
Stability and stabilization
H_∞-filtering
Linear matrix inequality (LMI)
Vehicle dynamics application

ABSTRACT

This paper considers the robust stability, stabilization and L_2-gain analysis of switched linear systems in the simultaneous presence of uncertain and exogenous disturbances inside subsystems. The control synthesis is performed by means of linear matrix inequalities (LMIs). The effectiveness of the proposed methods is tested and shown through lateral vehicle control application. Indeed, the simulation tests are conducted using experimental data previously recorded on a race track by an instrumented vehicle during several trials. Moreover, the stability of controlled and uncontrolled vehicle models is established by means of sideslip phase-plane criteria.

1. Introduction

Model-based methods have received an important consideration and remain an important tool to design control and estimation algorithms. Otherwise, the mathematical models of real systems are complex and affected by several parameter variations. To obtain simple and relevant models, many operating modes can be considered to describe such systems (Johansen, Shorten, & Murray-Smith, 2000). Therefore, a multiple model representation can easily be used. Consequently, the analysis and the synthesis of such systems involve the use of specific methods like adaptive methods (Narendra & Balakrishnan, 1997; Narendra, Driollet, Feiler, & George, 2003), gain-scheduled approaches (Apkarian, Gahinet, & Becker, 1995; Lawrence & Rugh, 1995; Leithead, 1999; Stilwell & Rugh, 1999), linear parameter varying systems (LPV) (Apkarian et al., 1995), Type-1 and Type-2 Fuzzy logic systems (Castillo & Melin, 2008; Mendel, 2004; Sugeno & Kang, 1988) and during the last decades the switched systems which constitute an important class of hybrid systems, have been introduced and widely developed (Branicky, 1998; Daafouz, Riedinger, & Iung, 2002; Deaecto, Geromel, & Daafouz, 2011; Geromel, Colaneri, & Bolzern, 2008; Koenig, Marx, & Jacquet, 2008; Koenig & Marx, 2009; Liberzon & Morse, 1999; Liberzon, 2003; Lin & Antsaklis, 2006, 2007, 2009; Narendra & Balakrishnan, 1994; Sun & Ge, 2005). Such systems are defined by a finite number of local operating modes and a logical rule that manages switching between them. The logical rule organizes switching between operating modes and generates switching signals. Generally, the operating modes may be described by a set of nonlinear and/or linear models.

Linear switched systems have been widely investigated in a large number of works and applied for many real systems. Particularly, stability and stabilization problems of switched continuous-time and discrete-time linear systems were addressed in Narendra and Balakrishnan (1994), Liberzon and Morse (1999), Sun and Ge (2005), Lin and Antsaklis (2007), Lin and Antsaklis (2009), Branicky (1998), Daafouz et al. (2002), Koenig et al. (2008) and Du, Jiang, Shi, and Zhou (2007). The stability of other switched systems was also investigated such as switched linear and nonlinear descriptor systems (Koenig et al., 2008; Koenig & Marx, 2009), switched discrete-time systems with constant and time-varying delays (Du et al., 2007; Wu & Zheng, 2009), and recently switched linear systems with singular perturbation (Deaecto, Daafouz, & Geromel, 2012; Hachemi, Sigalotti, & Daafouz, 2012). Moreover, the readers are referred to the large surveys (Lin & Antsaklis, 2009; Sun & Ge, 2005), which emphasize that the literature on design of such systems is abundant.

Based on the switched systems, the H_∞-filtering (Du et al., 2007; Xie, 1996) and the tracking state feedback control with a reference model, robust switched H_∞ controllers are developed. Here, based on a common Lyapunov function and switched Lyapunov functions approaches, the design problems are addressed in the discrete-time case. Their application is carried

* Corresponding author.
E-mail addresses: lghani.menhour@mines-paristech.fr (M. Lghani), Damien.Koenig@gispa-lab.grenoble-inp.fr (K. Damien), brigitte.dandrea-novel@mines-paristech.fr (d.-N. Brigitte).

http://dx.doi.org/10.1016/j.conengprac.2015.05.003
0967-0661/

out through a steering vehicle control. The lateral vehicle control problem is already addressed and published in several works (see Ackermann, Guldner, Sienel, Steinhauser, & Utkin, 1995; Cerone, Milanese, & Regruto, 2009; Marino & Cinili, 2009; Menhour, d'Andréa-Novel, Boussard, Fliess, & Mounier, 2011; Plochl & Edelmann, 2009 and the references therein). In many control studies, the vehicle models are assumed to be well known. However, this assumption is not consistent in practice particularly when the driving conditions become hard. In fact, all existing vehicle models are subjected to parameter variations and uncertainties. For example, as mentioned previously in Menhour, Koenig, and d'Andréa-Novel (2013a,b), longitudinal velocity and tire cornering stiffnesses are uncertain and vary over the time. Therefore, several solutions based on fuzzy systems (Chadli, Hajjaji, & Oudghiri, 2008; Manceur & Menhour, 2013; Menhour, Manceur, & Bouibed, 2012) and LPV systems (Fergani, Menhour, Sename, Dugard, & d'Andréa-Novel, 2013; Poussot-Vassal et al., 2011; Varrier, Koenig, & Martinez, 2014) are used to overcome such constraints. Moreover, the switched systems appears to be a powerful tool and good solution to deal with such a problem.

The remainder of this paper is organized as follows: Section 2 describes the linear two wheels vehicle model (LTWVM) and the problem statement of two robust switched controllers. Our main results concerning control design methods for switched uncertain linear systems are presented in Section 3. Other solutions for switched linear systems without uncertainties are also deduced. The simulation results with experimental data recorded previously by a laboratory vehicle are displayed in Section 4. Conclusions and perspectives are given in Section 5.

Notation 1. The superscript "T" stands for the transpose matrix; $\mathbb{R}^n$ denotes the n-dimensional Euclidean space and $P>0$ (≥ 0) denotes a symmetric positive definite matrix (semidefinite). In symmetric block matrices or complex matrix expressions, we use an asterisk ($*$) to represent a term that is induced by symmetry and $diag\{\cdots\}$ stands for a block-diagonal matrix. S H_∞ TSFC-CLF: Switched H_∞ Tracking State Feedback Controller based on Common Lyapunov Function, S H_∞ TSFC-SLF: Switched H_∞ Tracking State Feedback Controller based on Switched Lyapunov Function. NLFWVM: NonLinear Four Wheels Vehicle Model. LTWVM: Linear Two Wheels Vehicle Model.

2. Vehicle model and problem statement

The steering vehicle control problem based on switched systems is detailed in the sequel. We begin with the description of a linear two wheels vehicle model (see Fig. 1), then, by considering the parameter variations and uncertainties, it is transformed into a switched uncertain system. Thereafter, the control problem is addressed.

2.1. Bicycle vehicle model

For simplicity, the two degrees-of-freedom linear single track vehicle model is used (for notations, see Table 1). Assuming that the steering angle is small, the lateral and yaw dynamics including the road bank angle as unknown input are given by the following equations:

$$\begin{cases} ma_y = m(\dot{V}_y + \dot{\psi} V_x) = F_{yf} + F_{yr} - F_{bank} \\ I_z \ddot{\psi} = M_{zf} + M_{zr} \end{cases} \quad (1)$$

where $F_{bank} = mg\ \sin(\phi_r)$, by assuming that ϕ_r is relatively small, $F_{bank} \approx mg\phi_r$. The linear lateral tire forces are modeled as proportional to the sideslip angles ($F_{yf} = C_f\alpha_f$ and $F_{yr} = -C_r\alpha_r$) of each axle as follows:

$$\begin{cases} F_{yf} = C_f\left(\delta - \beta - \dfrac{L_f\dot{\psi}}{V_x}\right) \\ F_{yr} = -C_r\left(\beta - \dfrac{L_r\dot{\psi}}{V_x}\right) \end{cases} \quad (2)$$

and the yaw moments are given by

$$\begin{cases} M_{zf} = L_f F_{yf} \\ M_{zr} = -L_r F_{yr} \end{cases} \quad (3)$$

Table 1
Notations.

Symbol	Variable name
a_y	Lateral acceleration (m/s^2)
V_x	Longitudinal speed (m/s)
V_y	Lateral speeds (m/s)
ψ	Yaw angle (rad)
$\dot{\psi}$	Yaw rate (rad/s)
δ	Driver steering angle (rad)
ϕ_r	Road bank angle (rad)
β	Sideslip angle at center of gravity (rad)
F_{yf}, F_{yr}	Front and rear lateral forces in the vehicle coordinate (N)
M_{zf}, M_{zr}	Front and rear yaw moments (Nm)
L_f, L_r	Distances from the CoG to the front and rear axles (m)
I_z	Yaw moment of inertia (Kg m^{-2})
C_f, C_r	Front and rear cornering stiffnesses (N/rad)
α_f, α_r	Front and rear tire slip angle (rad)
g	Acceleration due to gravity (m/s^2)
m	Vehicle mass (kg)
y	Lateral deviation (m)
Y	System output (first derivative of the lateral deviation) (m/s)
$\dot{Y}$	Second derivative of the lateral deviation (m/s^2)
r	Reference input
f	Unknown input
σ_i	Switching signal
z	Premise variable

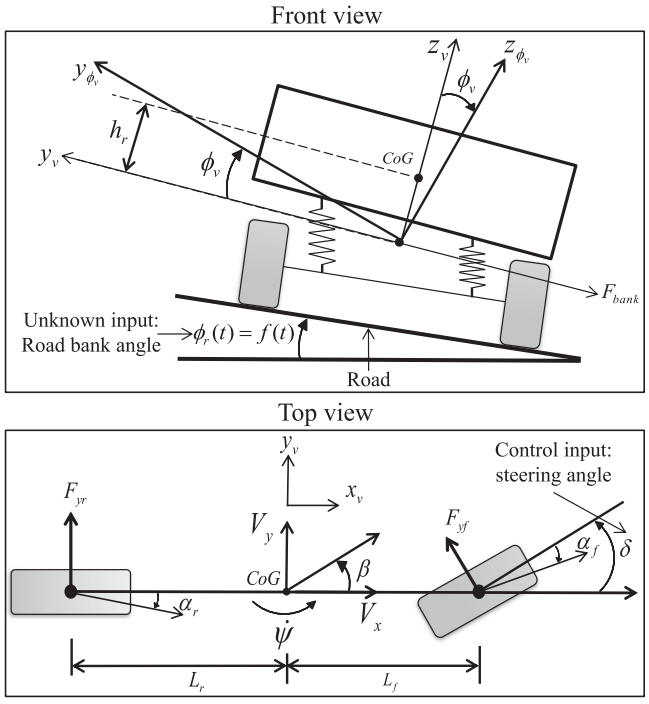

Fig. 1. Linear lateral vehicle model and its interaction with unknown input (road bank angle).

From (1)–(3), the following state space equations are obtained:

$$\begin{cases} \dot{X}(t) = AX(t) + Bu(t) + Ff(t) \\ Y(t) = CX(t) \end{cases} \tag{4}$$

where

$$X = \begin{bmatrix} V_y \\ \dot{\psi} \\ \psi \end{bmatrix}, \quad A = \begin{bmatrix} -\dfrac{2C_f + 2C_r}{mV_x} & -V_x - \dfrac{2C_fL_f - 2C_rL_r}{mV_x} & 0 \\ -\dfrac{2C_fL_f - 2C_rL_r}{I_zV_x} & -\dfrac{2C_fL_f^2 + 2C_rL_r^2}{mV_x} & 0 \\ 0 & 1 & 0 \end{bmatrix},$$

$$B = \begin{bmatrix} \frac{C_f}{m} \\ \frac{2L_fC_f}{I_z} \\ 0 \end{bmatrix}, \quad F = \begin{bmatrix} -g \\ 0 \\ 0 \end{bmatrix}$$

and $C = [1\ 0\ V_x]$. Here, $u(t) = \delta(t) \in \mathbb{R}^p$ is the control input (steering angle), $X(t) \in \mathbb{R}^n$ is the state vector, $Y(t) \in \mathbb{R}^m$ is the output (derivative of lateral deviation), $f(t) = \phi_r(t) \in \mathbb{R}^{n_f}$ is the unknown input (road bank angle) that satisfies $f \in L_2[0, \infty)$, and A, B, C and F are system matrices with appropriate size.

2.2. Problem statement

It is well known that the single-track vehicle model (4) is affected by parameter variations (like longitudinal speed $V_x(t)$ variation) and parametric uncertainties (like the uncertainties on the cornering stiffness coefficients C_f and C_r), then, such variations and uncertainties can be considered by using switched uncertain systems. In fact, the measured lateral tire characteristic during a braking maneuver (see Fig. 2) highlights two uncertainties on cornering stiffness coefficients $\Delta C_{(f,r)}$ around of a nominal dynamic $C_{(f,r)_0}$. Therefore, according to the characteristic of Fig. 2 the uncertain model can be used:

$$C_{(f,r)} = C_{(f,r)_0} + \Delta C_{(f,r)}$$

In order to consider simultaneously the parameter variations and the parametric uncertainties, we transform the Linear Time-Invariant (LTI) system (4) into a switched uncertain system as follows:

$$\begin{cases} \dot{X}(t) = \sum_{i=1}^{M} \sigma_i(z(t)) \{ [A_i + \Delta A_i(t)] X(t) + [B_i + \Delta B_i(t)] u(t) + F_i f(t) \} \\ Y(t) = \sum_{i=1}^{M} \sigma_i(z(t)) C_i X(t) \end{cases}$$

The function $\sigma_i(z(t))$ is the switching signal

$$\sigma_i : \mathbb{R}^+ \longrightarrow \{0,\ 1\} \quad \sum_{i=1}^{M} \sigma_i(z(t)) = 1, \quad t \in \mathbb{R}^+ \tag{5}$$

where $z(t)$ is the premise variable depending on measurable variable.

The matrices $\Delta A_i(t)$ and $\Delta B_i(t)$ represent the time varying parametric uncertainties of the following form:

$$\left\{ \begin{matrix} \Delta A_i(t) = H_i \Delta(t) E_{1_i} \\ \Delta B_i(t) = H_i \Delta(t) E_{2_i} \end{matrix} \right\} \Leftrightarrow [\Delta A_i(t), \Delta B_i(t)] = H_i \Delta(t) [E_{1_i} E_{2_i}] \tag{6}$$

with H_i, E_{1_i} and E_{2_i} are known matrices with appropriate dimension. $\Delta(t)$ is an unknown matrix function satisfying the following inequality:

$$\Delta^T(t)\Delta(t) \le I \tag{7}$$

The objective is to design simple switched H_∞ controllers, such that the state $X(t)$ of the closed-loop system tracks a given reference signal to satisfy the desired tracking performance. For this, we suppose that the reference state $X_r(t)$ may be computed by the following reference model:

$$\begin{cases} \dot{X}_r(t) = \sum_{i=1}^{M} \sigma_i(z(t)) [A_{r_i} X_r(t) + F_{r_i} r(t)] \\ Y_r(t) = \sum_{i=1}^{M} \sigma_i(z(t)) C_{r_i} X_r(t) \end{cases} \tag{8}$$

where $Y_r(t)$ has the same dimension as $Y(t)$. $X_r(t)$ and $r(t) \in \mathbb{R}^{n_r}$ are respectively the reference state and the bounded reference input. A_{r_i}, C_{r_i} and F_{r_i} are appropriately dimensioned with A_{r_i} Hurwitz. Notice that the control design procedure assumes that both $X(t)$ and $X_r(t)$ are measurable. For our purpose we define the following tracking output error:

$$\tilde{y}(t) = Y(t) - Y_r(t) \tag{9}$$

Therefore, the following augmented system is obtained:

$$\begin{cases} \dot{\xi}(t) = \sum_{i=1}^{M} \sigma_i(z(t)) \{ [A_{ai} + \Delta A_{ai}(t)] \xi(t) + [B_{ai} + \Delta B_{ai}(t)] u(t) + F_{ai} \omega(t) \} \\ \tilde{y}(t) = \sum_{i=1}^{M} \sigma_i(z(t)) C_{ai} \xi(t) \end{cases} \tag{10}$$

where

$$A_{ai} = \begin{bmatrix} A_i & 0 \\ 0 & A_{r_i} \end{bmatrix}, \quad B_{ai} = \begin{bmatrix} B_i \\ 0 \end{bmatrix}, \quad \Delta A_{ai} = \begin{bmatrix} \Delta A_{ai} & 0 \\ 0 & 0 \end{bmatrix},$$

$$\Delta B_{ai} = \begin{bmatrix} \Delta B_{ai} \\ 0 \end{bmatrix}, \quad F_{ai} = \begin{bmatrix} F_i & 0 \\ 0 & F_{r_i} \end{bmatrix}, \quad \xi(t) = \begin{bmatrix} X(t) \\ X_r(t) \end{bmatrix},$$

$$\omega(t) = \begin{bmatrix} f(t) \\ r(t) \end{bmatrix} \text{and } C_{ai} = \begin{bmatrix} C_i & -C_{r_i} \end{bmatrix}.$$

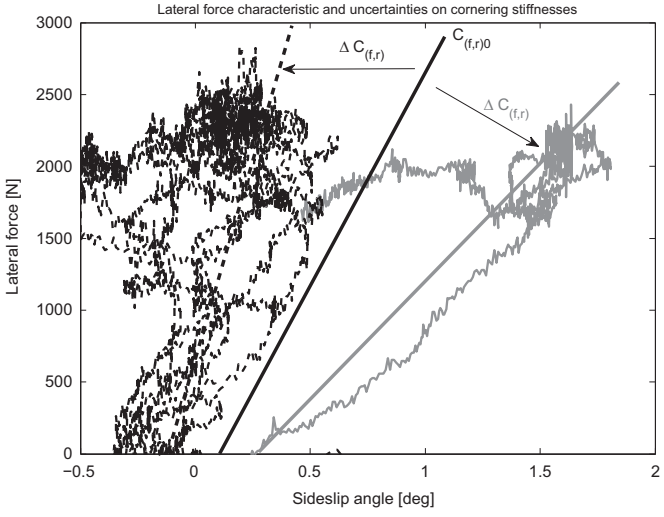

Fig. 2. Experimental braking maneuver: characteristic of the lateral tire force with uncertainties on cornering stiffnesses $\Delta C_{(f,r)}$.

The switched uncertain discrete-time system corresponding to model (10) using the first order Euler approximation is as follows:

$$\begin{cases} \xi_{k+1} = \sum_{i=1}^{M} \sigma_i(z_k)\left[\left(\overline{A}_{ai} + \overline{\Delta A}_{ai_k}\right)\xi_k + \left(\overline{B}_{ai} + \overline{\Delta B}_{ai_k}\right)u_k + \overline{F}_{ai}\omega_k\right] \\ \tilde{y}_k = \sum_{i=1}^{M} \sigma_i(z_k)\overline{C}_{ai}\xi_k \end{cases} \tag{11}$$

For this case, the functional switching rule $\sigma_i(z_k)$ is as follows:

$$\sigma_i : \mathbb{Z}^+ \longrightarrow \{0,\ 1\} \quad \sum_{i=1}^{M} \sigma_i(z_k) = 1, \quad k \in \mathbb{Z}^+ \tag{12}$$

with

$$\left[\overline{\Delta A}_{ai_k} \quad \overline{\Delta B}_{ai_k}\right] = \overline{H}_{ai}\Delta_k\left[\overline{E}_{1_{ai}} \quad \overline{E}_{2_{ai}}\right] \tag{13}$$

and

$$\Delta_k^T\Delta_k \le I \tag{14}$$

In the sequel, for switched uncertain system (11), a robust switched control problem is addressed.

Problem 1. Consider the following robust switched controller for switched uncertain system (11):

$$u_k = -\sum_{i=1}^{M} \sigma_i(z_k)\overline{K}_{ai}\xi_k \tag{15}$$

where the gains $\overline{K}_{ai} \in \mathbb{R}^{p\times n}$ are computed such that S1 and S2 are ensured.

S1. The closed-loop system $\xi_{k+1} = \sum_{i=1}^{M} \sigma_i(z_k)\left(\overline{A}_{ai} - \overline{B}_{ai}\overline{K}_{ai}\right)\xi_k$ is asymptotically stable when $\omega_k = 0$;
S2. The following optimization problem is feasible:

$$\begin{aligned} &\min \quad \gamma \\ &\text{subject to} \\ &\quad \|\overline{H}_{\tilde{y}\omega}(z)\|_\infty < \gamma \end{aligned} \tag{16}$$

where $\overline{H}_{\tilde{y}\omega}(z) = \sum_{i=1}^{M} \overline{C}_{ai}\left[zI - \left(\overline{A}_{ai} - \overline{B}_{ai}\overline{K}_{ai}\right)\right]^{-1}\overline{F}_{ai}$ is the transfer function, and $\|\overline{H}_{\tilde{y}\omega}(z)\|_\infty$ denotes the H_∞ norm from ω to $\tilde{y}$ for positive scalar γ.

Assumption 1. For control design procedure, we suppose that for $i \in \{1, \ldots, M\}$, the pairs $(\overline{A}_{ai},\ \overline{B}_{ai})$ are stabilizable.

Let us recall the following lemma and proposition commonly used in several works and which will be useful in the sequel.

Lemma 1. *Let $X = X^T > 0$, $N = N^T > 0$ and W be given matrices. By Schur complement, the following statements are equivalent:*

$$X - WN^{-1}W^T > 0 \Leftrightarrow \begin{pmatrix} X & W \\ W^T & N \end{pmatrix} > 0 \tag{17}$$

Proposition 1 (*Souza and Li, 1999*). *For any real matrices A, H, E and Δ with appropriate size and $\Delta^T\Delta \le I$, for any symmetric positive definite matrix P and a positive constant ϵ such that $P - \epsilon HH^T > 0$, we get*

$$(A + H\Delta E)^T P^{-1}(A + H\Delta E) \le A^T(P - \epsilon HH^T)^{-1}A + \epsilon^{-1}E^TE. \tag{18}$$

3. Robust switched H_∞ tracking state feedback controllers: discrete-time case

The robust stabilization with a pre-given L_2-gain for switched linear systems in the simultaneous presence of uncertainty and exogenous disturbance inside subsystems is presented in the following section. More precisely, two design methods for robust tracking state feedback controllers for switched uncertain linear system (11) are presented: firstly, using switched Lyapunov function, and secondly, using a common Lyapunov function.

3.1. Robust switched H_∞ tracking state feedback control: switched Lyapunov function design approach

The first objective is to determine the gains of (15) for (11) in order to stabilize the following closed-loop system:

$$\begin{cases} \xi_{k+1} = \sum_{i=1}^{M} \sigma_i(z_k)\left[\left((\overline{A}_{ai} + \overline{\Delta A}_{ai_k}) - (\overline{B}_{ai} + \overline{\Delta B}_{ai_k})\overline{K}_{ai}\right)\xi_k + \overline{F}_{ai}\omega_k\right] \\ \tilde{y}_k = \sum_{i=1}^{M} \sigma_i(z_k)\overline{C}_{ai}\xi_k \end{cases} \tag{19}$$

and satisfies S2. For this, we establish the following second theorem.

Theorem 1. *Under Assumption 1, if there exist constants $\gamma > 0$, $\epsilon > 0$, symmetric positive definite matrices $X_i, X_j \in \mathbb{R}^{(n+n_r)\times(n+n_r)}$ and matrices $U_{ai} \in \mathbb{R}^{m\times(n+n_r)}$ satisfying*

$$\min_{X_i,\ X_j,\ U_{ai}} \quad \gamma \tag{20}$$

subject to

$$\begin{bmatrix} -X_i & 0 & X_i\overline{A}_{ai}^T - U_{ai}^T\overline{B}_{ai}^T & X_i\overline{C}_{ai}^T & X_i\overline{E}_{1_{ai}} - U_{ai}^T\overline{E}_{2_{ai}}^T & 0 \\ * & -\gamma^2 I & \overline{F}_{ai}^T & 0 & 0 & 0 \\ * & * & -X_j & 0 & 0 & \overline{H}_{ai} \\ * & * & * & -I & 0 & 0 \\ * & * & * & * & -\epsilon I & 0 \\ * & * & * & * & * & -\epsilon^{-1}I \end{bmatrix} < 0 \tag{21}$$

for $(i,j) \in \{1, \ldots, M\}^2$, then, the gains of (15) are given by $\overline{K}_{ai} = U_{ai}X_i^{-1}$.

Proof. The sufficient conditions for the existence of (15) such that the closed-loop system (19) satisfies S1 and S2 are related to the existence of a switched Lyapunov function V_k such that the following inequality should be verified:

$$V_{k+1} - V_k + \tilde{y}_k^T\tilde{y}_k - \gamma^2\omega_k^T\omega_k < 0 \tag{22}$$

where

$$\begin{cases} V_k = \sum_{i=1}^{M} \sigma_i(z_k)\xi_k^T P_i\xi_k \\ V_{k+1} = \sum_{j=1}^{M} \sigma_j(z_{k+1})\xi_{k+1}^T P_j\xi_{k+1} \end{cases} \tag{23}$$

are the terms of the switched Lyapunov function. Then inequality (22) becomes

$$\sum_{j=1}^{M} \sigma_j(z_{k+1})\xi_{k+1}^T P_j\xi_{k+1} - \sum_{i=1}^{M} \sigma_i(z_k)\xi_k^T P_i\xi_k + \tilde{y}_k^T\tilde{y}_k - \gamma^2\omega_k^T\omega_k < 0 \tag{24}$$

To take into account all switches, the following cases are considered:

$$\begin{cases} \sigma_i(z_k) = 1 \quad \text{and} \quad \sigma_{l\neq i}(z_k) = 0 \\ \sigma_j(z_{k+1}) = 1 \quad \text{and} \quad \sigma_{l\neq j}(z_{k+1}) = 0 \end{cases} \tag{25}$$

Then, (19) and (24) are respectively equivalent to

$$\begin{cases} \xi_{k+1} = \left((\overline{A}_{ai}+\overline{\Delta A}_{ai_k})-(\overline{B}_{ai}+\overline{\Delta B}_{ai_k})\overline{K}_{ai}\right)\xi_k+\overline{F}_{ai}\omega_k \\ \tilde{y}_k = \overline{C}_{ai}\xi_k \end{cases} \tag{26}$$

and

$$\xi_{k+1}^T P_j \xi_{k+1} - \xi_k^T P_i \xi_k + \tilde{y}_k^T \tilde{y}_k - \gamma^2 \omega_k^T \omega_k < 0 \tag{27}$$

By computing (27) along system (26), we obtain

$$\begin{aligned} (27) \Leftrightarrow & \left[\left((\overline{A}_{ai}+\overline{\Delta A}_{ai_k})-(\overline{B}_{ai}+\overline{\Delta B}_{ai_k})\overline{K}_{ai}\right)\xi_k\right. \\ & \left.+\overline{F}_{ai}\omega_k\right]^T P_j \left[\left((\overline{A}_{ai}+\overline{\Delta A}_{ai_k})-(\overline{B}_{ai}+\overline{\Delta B}_{ai_k})\overline{K}_{ai}\right)\xi_k+\overline{F}_{ai}\omega_k\right] \\ & +\tilde{y}_k^T\tilde{y}_k-\gamma^2\omega_k^T\omega_k<0 \end{aligned} \tag{28}$$

which can be rewritten as

$$\begin{bmatrix} \xi_k \\ \omega_k \end{bmatrix}^T \begin{bmatrix} \Pi_{i,j}-P_i & \left((\overline{A}_{ai}+\overline{\Delta A}_{ai_k})-(\overline{B}_{ai}+\overline{\Delta B}_{ai_k})\overline{K}_{ai}\right)^T P_j \overline{F}_{ai} \\ \overline{F}_{ai}^T P_j \left((\overline{A}_{ai}+\overline{\Delta A}_{ai_k})-(\overline{B}_{ai}+\overline{\Delta B}_{ai_k})\overline{K}_{ai}\right) & -\gamma^2 I+\overline{F}_{ai}^T P_j \overline{F}_{ai} \end{bmatrix}$$

$$\begin{bmatrix} \xi_k \\ \omega_k \end{bmatrix} < 0 \tag{29}$$

where

$$\begin{aligned} \Pi_{i,j} = & \left((\overline{A}_{ai}+\overline{\Delta A}_{ai_k})-(\overline{B}_{ai}+\overline{\Delta B}_{ai_k})\overline{K}_{ai}\right)^T P_j \left((\overline{A}_{ai}+\overline{\Delta A}_{ai_k})\right. \\ & \left.-(\overline{B}_{ai}+\overline{\Delta B}_{ai_k})\overline{K}_{ai}\right)+\overline{C}_{ai}^T\overline{C}_{ai}. \end{aligned}$$

It follows that the difference $V_{k+1}-V_k$ is negative for any nonzero vector $[\xi_k \ \omega_k]$ if

$$\begin{bmatrix} \Pi_{i,j}-P_i & \left((\overline{A}_{ai}+\overline{\Delta A}_{ai_k})-(\overline{B}_{ai}+\overline{\Delta B}_{ai_k})\overline{K}_{ai}\right)^T P_j \overline{F}_{ai} \\ \overline{F}_{ai}^T P_j \left((\overline{A}_{ai}+\overline{\Delta A}_{ai_k})-(\overline{B}_{ai}+\overline{\Delta B}_{ai_k})\overline{K}_{ai}\right) & -\gamma^2 I+\overline{F}_{ai}^T P_j \overline{F}_{ai} \end{bmatrix} < 0 \tag{30}$$

From (13), (30) becomes

$$\left[\check{A}_{ai}+\check{H}_{ai}\Delta_k\check{E}_{ai}\right]^T \check{P}_j \left[\check{A}_{ai}+\check{H}_{ai}\Delta_k\check{E}_{ai}\right]-\check{P}_i<0 \tag{31}$$

with

$$\check{A}_{ai}=\begin{bmatrix} \overline{A}_{ai}^c & \overline{F}_{ai} \\ \overline{C}_{ai} & 0 \end{bmatrix}, \quad \check{P}_j=\begin{bmatrix} P_j & 0 \\ 0 & I \end{bmatrix}, \quad \check{P}_i=\begin{bmatrix} P_i & 0 \\ 0 & \gamma^2 I \end{bmatrix}, \quad \check{H}_{ai}=\begin{bmatrix} \overline{H}_{ai} \\ 0 \end{bmatrix},$$

$$\check{E}_{ai}=\begin{bmatrix} \overline{E}_{ai}^c & 0 \end{bmatrix}$$

and

$$\overline{A}_{ai}^c=\overline{A}_{ai}-\overline{B}_{ai}\overline{K}_{ai}$$
$$\overline{E}_{ai}^c=\overline{E}_{1_{ai}}-\overline{E}_{2_{ai}}\overline{K}_{ai}$$

Using Proposition 1, (31) becomes

$$\check{A}_{ai}^T\left[\check{P}_j^{-1}-\epsilon\check{H}_{ai}\check{H}_{ai}^T\right]^{-1}\check{A}_{ai}+\epsilon^{-1}\check{E}_{ai}^T\check{E}_{ai}-\check{P}_i<0 \tag{32}$$

Using Schur complement (17) twice, (32) becomes

$$\left[\begin{array}{cc|cc|cc} -P_i & 0 & \bar{A}_{ai}^{cT} & \bar{C}_{ai}^T & \bar{E}_{ai}^{cT} & 0 \\ 0 & -\gamma^2 I & \bar{F}_{ai}^T & 0 & 0 & 0 \\ \hline \bar{A}_{ai}^c & \bar{F}_{ai} & -P_j^{-1} & 0 & 0 & \bar{H}_{ai} \\ \bar{C}_{ai} & 0 & 0 & -I & 0 & 0 \\ \hline \multicolumn{2}{c|}{\bar{E}_{ai}^c \ \ 0} & \multicolumn{2}{c|}{0 \ \ 0} & -\varepsilon I & 0 \\ \multicolumn{2}{c|}{0 \ \ 0} & \multicolumn{2}{c|}{\bar{H}_{ai}^T \ \ 0} & 0 & -\varepsilon^{-1} I \end{array}\right] < 0 \tag{33}$$

Now, pre- and post-multiplying (33) by $diag(P_i^{-1}, I, I, I, I)$, (33) becomes

$$\begin{bmatrix} -P_i^{-1} & 0 & P_i^{-1}(\overline{A}_{ai}^T-\overline{K}_{ai}^T\overline{B}_{ai}^T) & P_i^{-1}\overline{C}_{ai}^T & P_i^{-1}(\overline{E}_{1_{ai}}-\overline{K}_{ai}^T\overline{E}_{2_{ai}}^T) & 0 \\ * & -\gamma^2 I & \overline{F}_{ai}^T & 0 & 0 & 0 \\ * & * & -P_j^{-1} & 0 & 0 & \overline{H}_{ai} \\ * & * & * & -I & 0 & 0 \\ * & * & * & * & -\epsilon I & 0 \\ * & * & * & * & * & -\epsilon^{-1} I \end{bmatrix} < 0 \tag{34}$$

Finally, substituting $X_i=P_i^{-1}$, $X_j=P_j^{-1}$ and $U_{ai}=\overline{K}_{ai}X_i$ into (34), leads to (21).□

3.2. Robust switched H_∞ tracking state feedback control: common Lyapunov function design approach

The second objective is to compute the gains of (15) for system (11) using a common Lyapunov function method. Based on Theorem 1 the following corollary is deduced.

Corollary 1. *Under* Assumption 1, *if there exist a constant* $\gamma>0$, *a scalar* $\epsilon>0$, *a common symmetric positive definite matrix* $X\in\mathbb{R}^{(n+n_r)\times(n+n_r)}$ *and matrices* $U_{ai}\in\mathbb{R}^{m\times(n+n_r)}$ *such that the following inequality is satisfied*

$$\begin{bmatrix} -X & 0 & X\overline{A}_{ai}^T-U_{ai}^T\overline{B}_{ai}^T & X\overline{C}_{ai}^T & X\overline{E}_{1_{ai}}-U_{ai}^T\overline{E}_{2_{ai}}^T & 0 \\ * & -\gamma^2 I & \overline{F}_{ai}^T & 0 & 0 & 0 \\ * & * & -X & 0 & 0 & \overline{H}_{ai} \\ * & * & * & -I & 0 & 0 \\ * & * & * & * & -\epsilon I & 0 \\ * & * & * & * & * & -\epsilon^{-1} I \end{bmatrix} < 0 \tag{35}$$

for $i\in\{1,\ldots,M\}$ *and* $X_j=X_i=X=P^{-1}$, *then, the gains* $\overline{K}_{ai}$ *of* (15) *are given by*

$$\overline{K}_{ai}=U_{ai}X^{-1}.$$

3.3. Switched H_∞ tracking state feedback controllers: discrete-time case

Note that if system (11) has no uncertainties ($\Delta A_i=0$ and $\Delta B_i=0$), the following results can be obtained from Theorem 1. Corollary 2 is deduced for switched Lyapunov functions, while Corollary 3 is deduced for a common Lyapunov function.

Corollary 2. *Under* Assumption 1, *and* $\Delta A_i=\Delta B_i=0$, *if there exist a constant* $\gamma>0$, *symmetric positive definite matrices* $X_i, X_j\in\mathbb{R}^{(n+n_r)\times(n+n_r)}$ *and matrices* $U_{ai}\in\mathbb{R}^{m\times(n+n_r)}$ *satisfying*

$$\begin{bmatrix} -X_i & 0 & X_i\overline{A}_{ai}^T-U_{ai}^T\overline{B}_{ai}^T & X_i\overline{C}_{ai}^T \\ * & -\gamma^2 I & \overline{F}_{ai}^T & 0 \\ * & * & -X_j & 0 \\ * & * & * & -I \end{bmatrix} < 0 \tag{36}$$

for $(i,j)\in\{1,\ldots,M\}^2$, then, the gains of (15) are given by

$$\overline{K}_{ai}=U_{ai}X_i^{-1}.$$

Corollary 3. *Under Assumption* 1, *and* $\Delta A_i=\Delta B_i=0$, *if there exist a constant* $\gamma>0$, *a common symmetric positive definite matrix* $X\in\mathbb{R}^{(n+n_r)\times(n+n_r)}$ *and matrices* $U_{ai}\in\mathbb{R}^{m\times(n+n_r)}$ *such that the inequality* (36) *is satisfied for* $i\in\{1,\ldots,M\}$ *and* $X_j=X_i=X=P^{-1}$, *then, the gains* $\overline{K}_{ai}$ *of* (15) *are given by* $\overline{K}_{ai}=U_{ai}X^{-1}$.

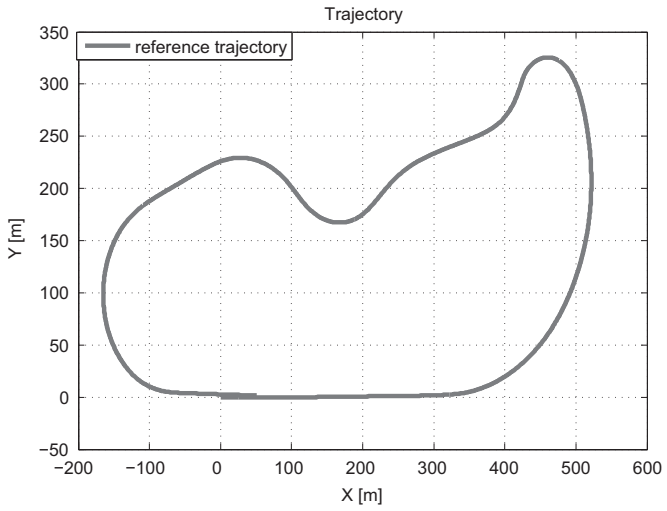

Fig. 3. Trajectory of the race track.

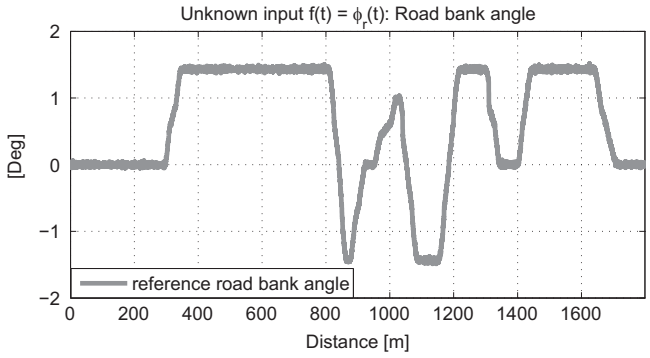

Fig. 4. Measured road bank angle considered as an unknown input.

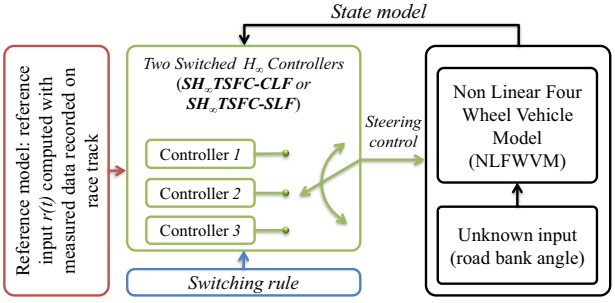

Fig. 5. A diagram block of the two switched H_∞ controllers coupled with vehicle model and reference model.

4. Simulation results using real data

The simulation tests with experimental data are given in this section. All used data are recorded previously by an instrumented Peugeot 406 vehicle on a real race track during an advanced experimentation campaign. The trajectory of the race track and its bank angle[1] are depicted in Figs. 3 and 4 respectively. Several trials are performed, for each of them, many dynamic parameters have been recorded at frequency 200 Hz; among the dynamical variables: longitudinal and lateral speeds, then sideslip angle, longitudinal and lateral accelerations, roll and pitch angles, yaw and roll rates, driver steering angle, wheel rotation speeds, longitudinal, lateral and vertical forces on four wheels, moments on four wheels, etc.

For our application, the reference model (8) describing the desired lateral deviation is given by

$$\begin{cases} \dot{X}_r(t) = -X_r(t) + r(t) \\ Y_r(t) = X_r(t) \end{cases} \tag{37}$$

where $r(t) = V_{x_r}(t)\sin(\psi_r(t)) + V_{y_r}(t)\cos(\psi_r(t)) + a_{y_r}(t)$, $A_r = -1$, $F_r = 1$ and $C_r = 1$. The reference input $r(t)$ is computed with recorded data. Fig. 5 displays the validation scheme with three specific parts: reference model, two discrete switched controllers (S H_∞ TSFC-CLF and S H_∞ TSFC-SLF), and nonlinear vehicle model. In fact, the simulation results given here are conducted using a full non-linear four wheels vehicle model (NLFWVM) (Menhour, d'Andréa-Novel, Fliess, & Mounier, 2014) of a Peugeot 406 vehicle. Such a model is composed of 10 Degrees-of-freedom which are: longitudinal V_x, lateral V_y and vertical V_z translational motions, roll ϕ, pitch θ and yaw ψ rotational motions and dynamical models of the four wheels. All these motions are described by the following model:

$$\begin{cases} m(\dot{V}_x + V_z\dot{\theta} - \psi V_y) & = \sum_{i=1}^{4} F_{xi} - F_{aero_x} + mg\sin(\phi_r - \theta_r) + m_s h\psi\phi \\ m(\dot{V}_y + \psi V_x - V_z\dot{\phi}) & = \sum_{i=1}^{4} F_{yi} - F_{aero_y} - mg\sin(\theta_r - \phi_r)\cos(\phi_r - \theta_r) - m_s h\ddot{\phi} \\ m(\dot{V}_z + V_y\dot{\phi} - V_x\dot{\theta}) & = F_{z1} + F_{z2} + F_{z3} + F_{z4} - mg \\ (I_x + mh^2)\ddot{\phi} & = I_{xz}\ddot{\psi} + [m_s gh - (K_{\phi f} + K_{\phi r})]\phi - (C_{\phi f} + C_{\phi r})\dot{\phi} - m_s h(\dot{V}_y V_x\psi) \\ I_y\ddot{\theta} & = (F_{z1} + F_{z2})L_1 + (F_{z3} + F_{z4})L_2 - \sum_{i=1}^{4} h_i F_{xi} + (I_z - I_x)\psi\dot{\phi} \\ I_z\ddot{\psi} - I_{xz}\ddot{\phi} & = M_{z1} + M_{z2} + M_{z3} + M_{z4} + \sum_{i=1}^{4} C_{zi} \\ I_\omega\dot{\omega}_i & = T_{\omega i} - RF_{x\omega i} \quad \text{for } i = 1, \ldots, 4 \end{cases} \tag{38}$$

A realistic vehicle behavior is achieved through good choices of longitudinal and lateral tire models. For this, a coupled nonlinear tire model (Pacejka, 2005) is used. It takes into account the coupling of longitudinal slip ratio, lateral slip angles, vertical forces and camber angles. The nonlinear longitudinal and lateral tire models can be expressed as follows:

$$F_{(x,y)\omega i} = f_{(x,y)i}(\zeta_i, \lambda_i, \alpha_i, F_{zi}) \quad \text{for} \quad i = 1, \ldots, 4 \tag{39}$$

and

$$\begin{pmatrix} F_{xi} \\ F_{yi} \end{pmatrix} = \begin{pmatrix} \cos\delta_i & -\sin\delta_i \\ \sin\delta_i & \cos\delta_i \end{pmatrix} \begin{pmatrix} F_{x\omega i} \\ F_{y\omega i} \end{pmatrix}$$

The above vehicle model is clearly more complex than the one used for control design (4).

Remark 1. It should be pointed out that the yaw rate is measured by a gyrometer sensor and the yaw angle can easily be deduced from the road curvature over the path length coordinate. Concerning the lateral speed it can be estimated using robust observers and the measured yaw rate, steering angle, odometer data which are available on commercialized vehicles (see for example Villagra, d'Andréa-Novel, Fliess, & Mounier, 2011).

The performances of the two robust switched controllers are highlighted through longitudinal speed variation. For this, three values ($V_{x_1} = 33$ km/h, $V_{x_2} = 66$ km/h and $V_{x_3} = 99$ km/h) are

[1] It should be noted that the road bank angle $f = \phi_r$ is used as unknown input and its spectral domain is located in a low frequency range.

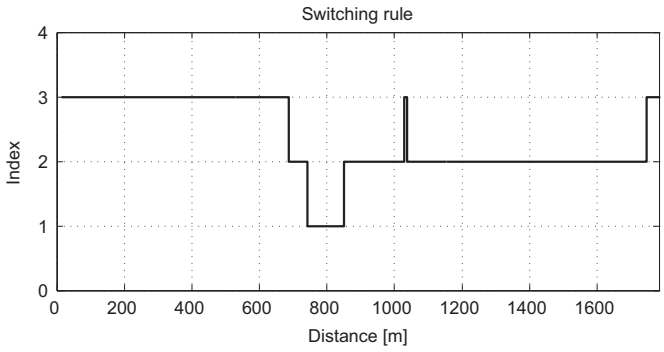

Fig. 7. Switching rule of our simulation test.

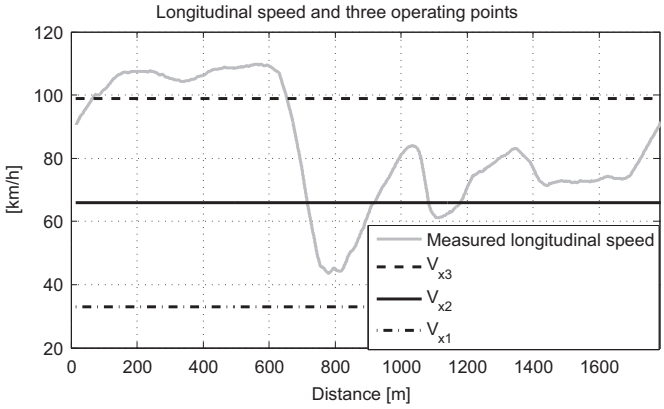

Fig. 6. Measured longitudinal speed with three operating points.

chosen to define the switching rules:

$$\begin{cases} i=1 \quad \text{and} \quad V_x = V_{x_1} & \text{If } z \in [V_{x_1}-\Delta,\ \Delta+V_{x_1}[\\ i=2 \quad \text{and} \quad V_x = V_{x_2} & \text{If } z \in [V_{x_2}-\Delta,\ \Delta+V_{x_2}[\\ i=3 \quad \text{and} \quad V_x = V_{x_3} & \text{If } z \in [V_{x_3}-\Delta,\ \Delta+V_{x_3}[\end{cases} \tag{40}$$

with $\Delta=(V_{x_{l+1}}-V_{x_l})/2$ for $l=1,\ldots,2$. The application of (40) on our simulation case gives the switching signal depicted in Fig. 7 and the corresponding longitudinal speed is shown in Fig. 6. Consequently, a set of three models are obtained ($M=3$ and $(i,j)\in\{1,2,3\}^2$). The stability resulting from the two switched controllers (15) is guaranteed by solving 3 LMIs of Corollaries 1 and 9 LMIs of Theorem 1 to obtain a common Lyapunov matrix P and three Lyapunov matrices (P_1, P_2 and P_3) respectively. Moreover, the uncertainties of 30% on C_f and C_r are considered for control design and $H_i=I$. All LMI constraints are solved using YALMIP software (Löfberg, 2004), then, after some iterations, we find

$$\overline{K}_{a1}=\begin{bmatrix}0.0717 & 2.8273 & 2.6371 & -3.4688\end{bmatrix}$$

$$\overline{K}_{a2}=\begin{bmatrix}0.1116 & 2.9238 & 2.8174 & -3.3199\end{bmatrix}$$

$$\overline{K}_{a3}=\begin{bmatrix}0.0810 & 3.0585 & 2.7428 & -3.4629\end{bmatrix}$$

using Theorem 1, and

$$\overline{K}_{a1}=\begin{bmatrix}0.0231 & 0.3565 & 0.5212 & -1.3918\end{bmatrix}$$

$$\overline{K}_{a2}=\begin{bmatrix}0.0359 & 0.3687 & 0.5568 & -1.3320\end{bmatrix}$$

$$\overline{K}_{a3}=\begin{bmatrix}0.0261 & 0.3857 & 0.5420 & -1.3894\end{bmatrix}$$

using Corollary 1. The H_∞ performances are guaranteed for $\gamma^*=1.8$.

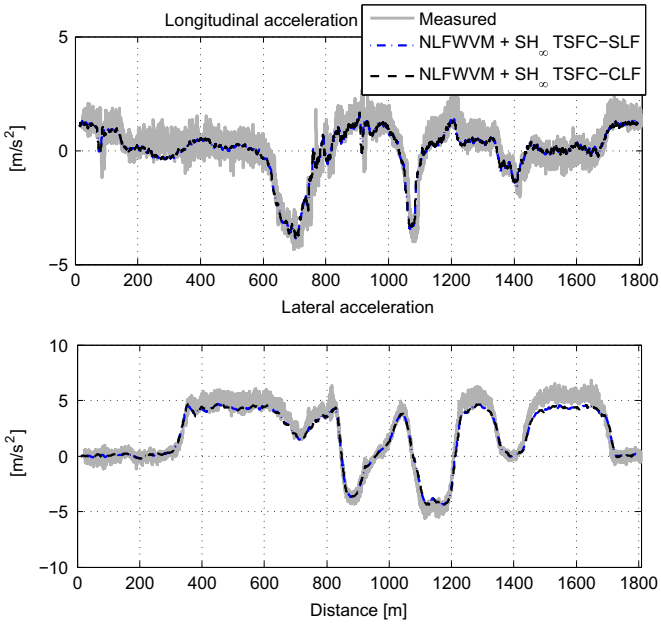

Fig. 8. Longitudinal and lateral accelerations: measured and computed by controlled non-linear vehicle models.

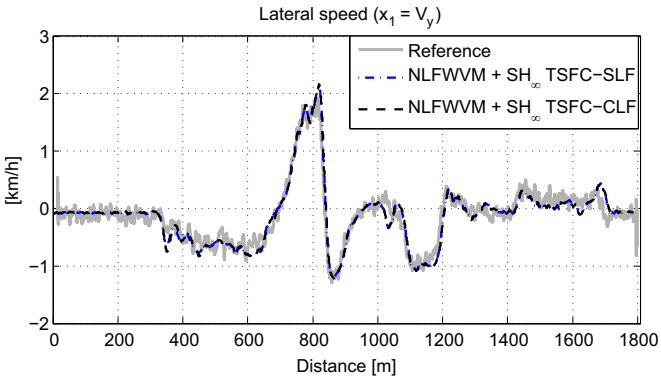

Fig. 9. Closed-loop system lateral speeds (first state $X_1=V_y$) using the robust switched controllers: reference and computed by controlled non-linear vehicle models.

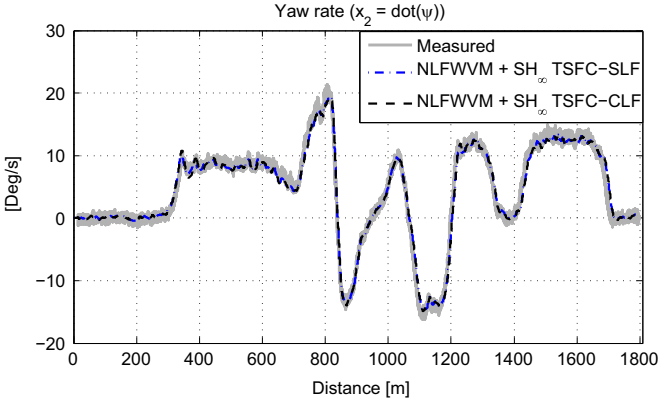

Fig. 10. Closed-loop system yaw rate (second state $X_2=\dot{\psi}$) using the robust switched controllers: reference and computed by controlled non-linear vehicle models.

Figs. 8–12 depict the longitudinal and lateral dynamical behaviors of the vehicle, while Figs. 13 and 14 display the trajectories and tracking errors. Moreover, the main dynamical variables depicted on these figures are: longitudinal and lateral

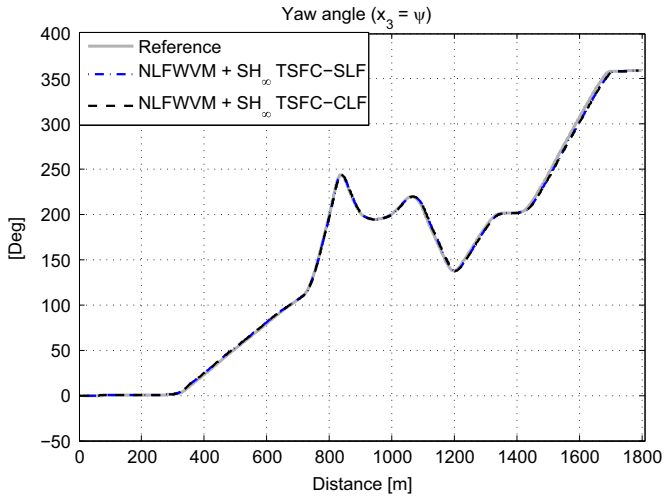

Fig. 11. Closed-loop system yaw angle (third state $X_3 = \psi$) using the robust switched controllers: reference and computed by controlled non-linear vehicle models.

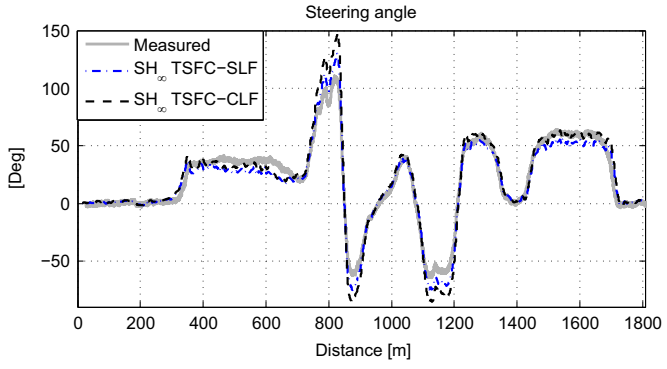

Fig. 12. Steering angle control: reference driver steering angle and steering angle computed by two controllers coupled with NLFWVM.

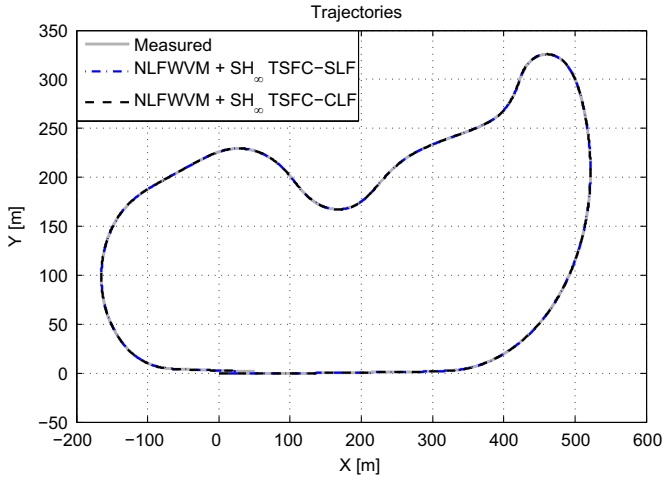

Fig. 13. Closed-loop system $(x-y)$ trajectories using the robust switched controllers: reference and those of controlled non-linear vehicle models.

accelerations, yaw rate, lateral speed, yaw angle, driver steering angle, $X-Y$ trajectories and tracking errors. We can observe that the closed-loop simulations results are close to the actual ones.

These results confirm the ability of the proposed controllers to track straight or curved trajectories as displayed in Fig. 13. Furthermore, the tracking errors on lateral deviation and yaw angle displayed in Fig. 14 are quite small and satisfactory. In fact, the tracking errors are less than 2.5° and 0.2 m for yaw angle and lateral deviation respectively. However, we can observe that the tracking errors obtained with S H_∞ TSFC-SLF are less than those obtained with S H_∞ TSFC-CLF, this may be due to the use of the Common Lyapunov Function (Corollary 1).

It is well known that the vehicle stability can easily be studied through the vehicle's sideslip motion. To have a stable vehicle, such a dynamics must stay in the stability region of the sideslip phase-plane $(\beta, \dot{\beta})$. The aim is therefore to maintain the sideslip motion within the stability region, and outside this region, the vehicle becomes unstable. The phase-plane $(\beta, \dot{\beta})$ stability approach commonly used in literature (He, Crolla, Levesley, & Manning, 2006; Koibuchi, Yamamoto, & Inagaki, 1996), is employed here to evaluate the stability of controlled and uncontrolled non-linear vehicle models. This criteria as defined and used

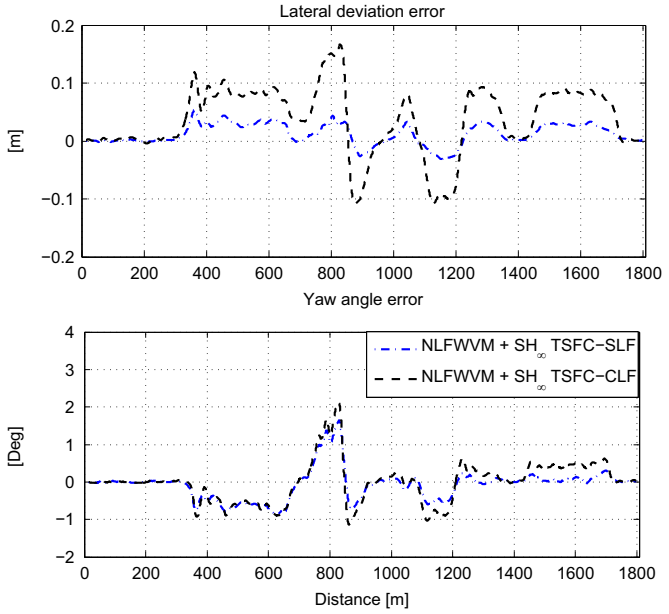

Fig. 14. Tracking trajectory errors on lateral deviation and yaw angle of controlled non-linear vehicle models.

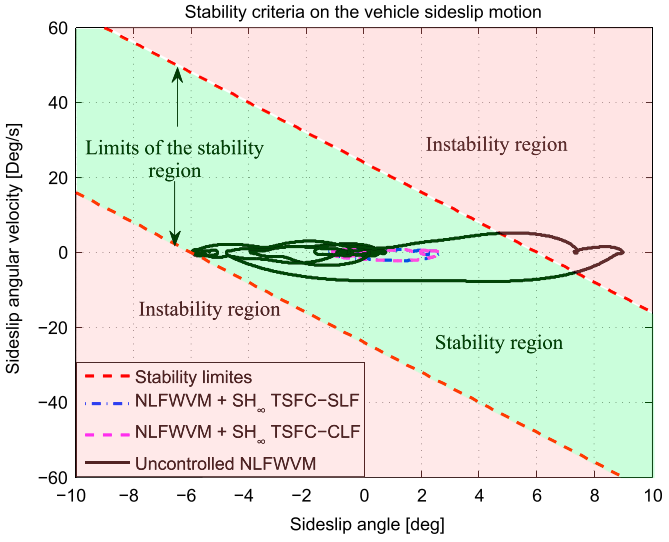

Fig. 15. Stability evolution of the controlled and uncontrolled vehicle models in the β–$\dot{\beta}$ plane.

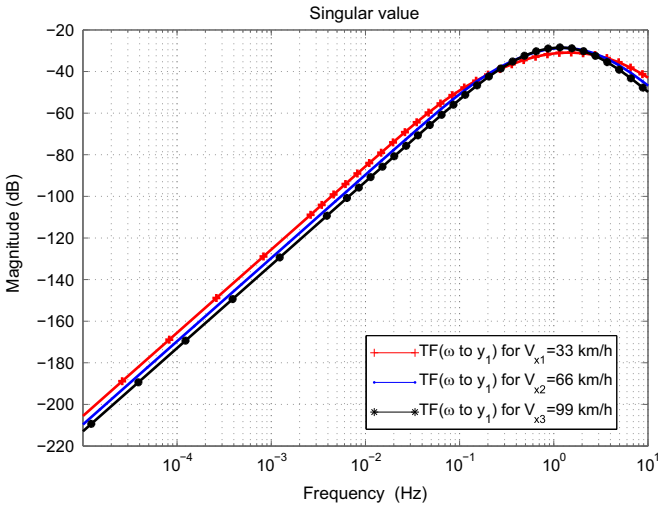

Fig. 16. Transfer function of subsystems $((\overline{A}_{ai}-\overline{B}_{ai}K_{ai}^{d}), \overline{F}_{ai}, \overline{C}_{ai})$ for three values $V_{x1}=33$ km/h and $V_{x2}=66$ km/h and $V_x=99$ km/h, between ω and $\tilde{y}$.

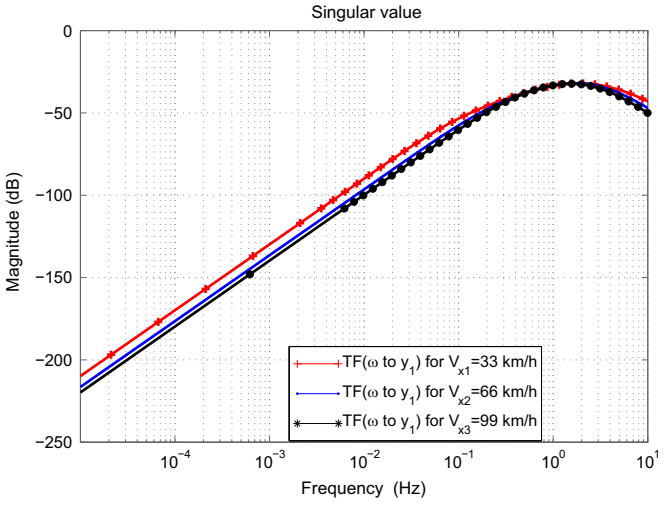

Fig. 17. Transfer function of subsystems $((\overline{A}_{ai}-\overline{B}_{ai}\overline{K}_{ai}), \overline{F}_{ai}, \overline{C}_{ai})$ for three values $V_{x1}=33$ km/h and $V_{x2}=66$ km/h and $V_x=99$ km/h, between ω and $\tilde{y}$.

in He et al. (2006) and Koibuchi et al. (1996) is the following:

$$\left|\frac{4}{24}\beta+\frac{1}{24}\dot{\beta}\right|<1 \tag{41}$$

The stability analysis of the sideslip motion of the controlled and uncontrolled vehicle models is shown in Fig. 15. We can observe that the sideslip behavior of the controlled vehicle models remains inside the stability region, however, the uncontrolled ones operates outside this region. These results confirm also the ability of the proposed controllers to keep the vehicle models more stable. It should be pointed out that the uncontrolled vehicle model is simulated in open-loop with measured driver steering angle and no control law.

Furthermore, Figs. 16 and 17 show the unknown input attenuation properties of subsystems $((\overline{A}_{ai}-\overline{B}_{ai}K_{ai}^{d}), \overline{F}_{ai}, \overline{C}_{ai})$ for a common Lyapunov function method and $((\overline{A}_{ai}-\overline{B}_{ai}\overline{K}_{ai}), \overline{F}_{ai}, \overline{C}_{ai})$ for switched Lyapunov function method, between ω and $\tilde{y}$ respectively.

Moreover, the UI attenuation is also confirmed by computing $\|\omega\|_2=\|f\|_2+\|r\|_2$ and $\|\tilde{y}\|_2$, which results for a common Lyapunov function method to

$$\frac{\|\tilde{y}\|_2}{\|\omega\|_2}=0.0082<\gamma^*=1.8 \tag{42}$$

and for switched Lyapunov function method to

$$\frac{\|\tilde{y}\|_2}{\|\omega\|_2}=0.0042<\gamma^*=1.8 \tag{43}$$

these results confirm the effectiveness of the two proposed control methods.

5. Conclusion

Two design methods for robust switched H_∞ tracking state feedback controllers are proposed. These methods are constructed around of a common Lyapunov function and switched Lyapunov functions approaches. All sufficient conditions for the existence of two robust controllers are obtained and given in terms of linear matrix inequalities (LMIs). Thus, the design of such controllers is reduced to the solving of LMI constraints using YALMIP software (Löfberg, 2004). The performance of the proposed methods is demonstrated through the steering vehicle control application. The simulations results are obtained with recorded experimental data. All data are recorded previously on real race track with an instrumented Peugeot 406 car.

For the illustrative example, the switching rule is constructed around the measured longitudinal speed, thereafter, in order to improve the performance and the effectiveness of such controllers, it will be interesting to investigate and define a new switching rule based on tire cornering stiffnesses C_f and C_r.

Acknowledgements

The authors would like to thank the anonymous reviewers for their valuable comments about the paper.

References

Ackermann, J., Guldner, J., Sienel, W., Steinhauser, R., & Utkin, V. I. (1995). Linear and nonlinear controller design for robust automatic steering. *IEEE Transactions on Control Systems Technology*, *3*(1), 132–143.

Apkarian, P., Gahinet, P., & Becker, G. (1995). Self-scheduled H_∞ control of linear parameter-varying systems: A design example. *Automatica*, *31*(9), 1251–1261.

Branicky, M. (1998). Multiple Lyapunov functions and other analysis tools for switched and hybrid systems. *IEEE Transactions on Automatic Control*, *43*(4), 475–482.

Castillo, O., & Melin, P. (2008). *Type-2 fuzzy logic: Theory and applications*. Berlin, Heidelberg: Springer-Verlag.

Cerone, V., Milanese, M., & Regruto, D. (2009). Combined automatic lane-keeping and driver's steering through a 2-DOF control strategy. *IEEE Transactions on Control Systems Technology*, *17*(1), 135–142.

Chadli, M., Hajjaji, A. E., & Oudghiri, M. (2008). Robust output fuzzy control for vehicle lateral dynamic stability improvement. *International Journal of Modelling, Identification and Control*, *3*(3), 247–257.

Daafouz, J., Riedinger, P., & Iung, C. (2002). Stability analysis and control synthesis for switched systems: A switched Lyapunov function approach. *IEEE Transactions on Automatic Control*, *47*(11), 1883–1887.

Deaecto, G. S., Daafouz, J., & Geromel, J. C. (2012). H_2 and H_∞ performance optimization of singularly perturbed switched systems. *SIAM Journal on Control and Optimization*, *50*(3), 1597–1615.

Deaecto, G. S., Geromel, J. C., & Daafouz, J. (2011). Dynamic output feedback H_∞ control of switched linear systems. *Automatica*, *47*(8), 1713–1720.

Du, D., Jiang, B., Shi, P., & Zhou, S. (2007). H_∞ filtering of discrete-time switched systems with state delays via switched Lyapunov function approach. *IEEE Transactions on Automatic Control*, *52*(8), 1520–1525.

Fergani, S., Menhour, L., Sename, O., Dugard, & L., d'Andréa-Novel, B., (2013). A new LPV/H_∞ semi-active suspension control strategy with performance adaptation to roll behavior based on non linear algebraic road profile estimation. *IEEE conference on decision and control*. Florence, Italy.

Geromel, J. C., Colaneri, P., & Bolzern, P. (2008). Dynamic output feedback control of switched linear systems. *IEEE Transactions on Automatic Control*, *53*, 720–733.

Hachemi, F. E., Sigalotti, M., & Daafouz, J. (2012). Stability analysis of singularly perturbed switched linear systems. *IEEE Transactions on Automatic Control*, *57*(8), 2116–2121.

He, J., Crolla, D. A., Levesley, M. C., & Manning, W. J. (2006). Coordination of active steering, driveline, and braking for integrated vehicle dynamics control. *IMechE Journal on Automobile Engineering*, *220*, 1401–1421.

Johansen, T., Shorten, R., & Murray-Smith, R. (2000). On the interpretation and identification of dynamic Takagi–Sugeno fuzzy models. *IEEE Transactions on Fuzzy Systems*, *8*(3), 297–313.

Koenig, D., & Marx, B. (2009). H_∞ filtering and state feedback control for discrete-time switched descriptor systems. *IET Control Theory and Applications*, *3*(6), 661–670.

Koenig, D., Marx, B., & Jacquet, D. (2008). Unknown input observers for switched nonlinear discrete time descriptor systems. *IEEE Transactions on Automatic Control*, *53*(1), 373–379.

Koibuchi, K., Yamamoto, & M., Inagaki, S. (1996). Vehicle stability in limit cornening by active brake. *SAE International*. February 26–29. Michigan.

Lawrence, D. A., & Rugh, W. J. (1995). Gain-scheduling dynamic linear controllers for a nonlinear plant. *Automatica*, *31*(3), 381–390.

Leithead, W. (1999). Survey of gain-scheduling analysis and design. *International Journal of Control*, *73*, 1001–1025.

Liberzon, D. (2003). *Switching in systems and control*. Boston: Birkhäuser.

Liberzon, D., & Morse, A. S. (1999). Basic problems in stability and design of switched system. *IEEE Control Systems Magazine*, *19*(5), 59–70.

Lin, H., & Antsaklis, P. J. (2006). Switching stabilization and L_2 gain performance controller synthesis for discrete-time switched linear systems. *Proceedings of the 45th IEEE conference on decision control* (pp. 2673–2678).

Lin, H., & Antsaklis, P. J. (2007). Switching stabilizability for continuous-time uncertain switched linear systems. *IEEE Transactions on Automatic Control*, *52*(4), 633–646.

Lin, H., & Antsaklis, P. J. (2009). Stability and stabilizability of switched linear systems: A survey of recent results. *IEEE Transactions on Automatic Control*, *54*(2), 308–322.

Löfberg, J. (2004). Yalmip: A toolbox for modeling and optimization in MATLAB. *Proceedings of the CACSD conference*. Taipei, Taiwan. ⟨http://users.isy.liu.se/johanl/yalmip⟩.

Manceur, M., & Menhour, L. (2013). Higher order sliding mode controller for driving steering vehicle wheels: Tracking trajectory problem. *IEEE conference on decision and control*. Florence, Italy.

Marino, R., & Cinili, F. (2009). Input–output decoupling control by measurement feedback in four wheel-steering-vehicles. *IEEE Transactions on Control Systems Technology*, *17*, 1163–1172.

Mendel, J. (2004). Computing derivatives in interval type-2 fuzzy logic systems. *IEEE Transactions on Fuzzy Systems*, *12*(1), 84–98.

Menhour, L., d'Andréa-Novel, B., Boussard, C., Fliess, M., & Mounier, H. (2011). Algebraic nonlinear estimation and flatness-based lateral/longitudinal control for automotive vehicles. *14th International IEEE conference on ITS*. Washington. Available at: ⟨http://hal.inria.fr/hal-00611950/⟩.

Menhour, L., d'Andréa-Novel, B., Fliess, M., & Mounier, H. (2014). Coupled nonlinear vehicle control: *Flatness-based setting with algebraic estimation techniques*. *Control Engineering Practice*, *22*(0), 135–146.

Menhour, L., Koenig, D., & d'Andréa-Novel, B. (2013a). Continuous-time and discrete-time switched H_∞ state feedback controllers: Application for a robust steering vehicle control. *Proceedings of the European control conference (ECC)*. Switzerland, Zurich, July 17–19.

Menhour, L., Koenig, D., & d'Andréa-Novel, B. (2013b). Functional switched H_∞ proportional integral observer applied for road bank and vehicle roll angles estimation. *IEEE international conference on networking sensing and control (IEEE-ICNSC 13)*. Paris, France.

Menhour, L., Manceur, M., & Bouibed, K. (2012). First order sliding fuzzy interval type-2 control applied for the steering vehicle control. *IEEE SMC*. Seoul, Korea.

Narendra, K. S., & Balakrishnan, J. (1994). A common Lyapunov function for stable LTI systems with commuting A-matrices. *IEEE Transactions on Automatic Control*, *39*, 2469–2471.

Narendra, K. S., & Balakrishnan, J. (1997). Adaptive control using multiple models. *IEEE Transactions on Automatic Control*, *42*(February (2)), 171–187.

Narendra, K. S., Driollet, O. A., Feiler, M., & George, K. (2003). Adaptive control using multiple models, switching and tuning. *International Journal of Adaptive Control and Signal Processing, Special Issue: Multiple models in adaptive systems*, *17*(March (2)), 87–102.

Pacejka, H. B. (2005). *Tire and vehicle dynamics*. Netherlands: Elsevier.

Plochl, M., & Edelmann, J. (2009). Driver models in automobile dynamics application. *Vehicle System Dynamics*, *45*(7–8), 699–741.

Poussot-Vassal, C., Sename, O., Dugard, L., Gaspar, P., Szaboc, Z., & Bokor, J. (2011). Attitude and handling improvements through gain-scheduled suspensions and brakes control. *Control Engineering Practice*, *19*, 252–263.

Souza, C.-E. D., & Li, X. (1999). Delay-dependent robust H_∞ control of uncertain linear state-delayed systems. *Automatica*, *35*, 1313–1321.

Stilwell, D. J., & Rugh, W. J. (1999). Interpolation of observer state feedback controllers for gain scheduling. *IEEE Transactions on Automatic Control*, *44*(6), 1225–1229.

Sugeno, M., & Kang, G. (1988). Structure identification of fuzzy model. *Fuzzy Sets and Systems*, *28*(1), 15–33.

Sun, Z., & Ge, S. S. (2005). Analysis and synthesis of switched linear control systems. *Automatica*, *41*(2), 181–195.

Varrier, S., Koenig, D., & Martinez, J. (2014). Robust fault detection for uncertain unknown inputs LPV system. *Control Engineering Practice*, *22*(0), 125–134.

Villagra, J., d'Andréa-Novel, B., Fliess, & M., Mounier, H. (2011). A diagnosis-based approach for tire-road forces and maximum friction estimation. Control Engineering Practice, 19, 174–184. Available at: ⟨http://hal.inria.fr/inria-00533586/⟩.

Wu, L., & Zheng, W. X. (2009). Weighted H_∞ model reduction for linear switched systems with time-varying delay. *Automatica*, *45*(1), 186–193.

Xie, L. (1996). Output feedback H_∞ control of systems with parameter uncertainty. *Int. J. Control*, *63*(4), 741–750.